Book of Tutorials and Abstracts

European
Microbeam Analysis Society

University of BRISTOL

Mineralogical Society

EMAS 2018

13th EMAS Regional Workshop

MICROBEAM ANALYSIS IN THE EARTH SCIENCES

4 - 7 September 2018

University of Bristol, Wills Hall, Bristol, Great Britain

Organised in collaboration with:
Mineralogical Society of Great Britain and Ireland
and
University of Bristol

HIGH-ANGULAR RESOLUTION ELECTRON BACKSCATTER DIFFRACTION AS A NEW TOOL FOR MAPPING LATTICE DISTORTION IN GEOLOGICAL MATERIALS

D. Wallis

Utrecht University, Department of Earth Sciences
3584 CB Utrecht, The Netherlands
e-mail: d.wallis@uu.nl

David Wallis received his MSc degree (2010) from the University of Durham and PhD (2014) from the University of Leeds. His PhD-research, under the supervision of Dr. Richard Phillips and Dr. Geoff Lloyd, focussed on relating the structure and microstructure of the Karakoram Fault, NW India, to its mechanical behaviour and role in the India-Asia collision. Subsequently, David worked as a Postdoctoral Research Assistant (2015-2017) at the University of Oxford in the Rock Rheology lab of Dr. Lars Hansen (Department of Earth Sciences) and Micromechanics group of Prof. Angus Wilkinson (Department of Materials). This work involved adapting and applying the technique of high-angular resolution electron backscatter diffraction (HR-EBSD), developed largely by the Micromechanics group, to geological materials. David applied the technique to minerals deformed in both experimental and natural contexts to gain insights into their deformation mechanisms and rheological behaviours. In 2017, David was appointed as Assistant Professor at Utrecht University in the Structural Geology and Electron Microscopy Group led by Prof. Martyn Drury. At Utrecht, David continues to develop the application of HR-EBSD to geological materials, with a particular focus on the microstructures formed by dislocation-mediated deformation at high temperatures.

ABSTRACT

Electron backscatter diffraction (EBSD) in the scanning electron microscope has become central to microstructural analysis in a wide range of geoscience subdisciplines. In particular, EBSD is employed intensively to investigate the microstructures of deformed rocks. However, conventional EBSD, based on indexing the Hough transform of each diffraction pattern, reveals only a fraction of the information on intragranular deformation that is stored in each pattern. Recent work in the materials sciences has generated a new approach to analysing diffraction patterns based on cross correlation of multiple regions of interest between patterns. This method, termed high-angular resolution electron backscatter diffraction (HR-EBSD), offers several advantages over conventional EBSD for analysis of intragranular lattice distortions. The cross-correlation based approach improves precision in misorientation angles by approximately an order of magnitude to around 0.01°. This precision allows lower densities of geometrically necessary dislocations to be resolved. Moreover, the associated misorientation axes are much better constrained, even for small misorientation angles. These improved constraints aid determination of the types of dislocations that generate lattice curvature. A further major advantage of HR-EBSD is that it maps elastic strain of the lattice, which is not analysed at all by conventional EBSD, with precision on the order of 10^{-4}. These measurements are relative to the strain state of a reference point within each grain and therefore quantify intragranular strain heterogeneity. With knowledge of the elastic constants, the strains are used to calculate intragranular residual stress heterogeneity, with precision on the order of tens of megapascals. Simple examples of HR-EBSD datasets from experimentally deformed olivine and naturally deformed quartz demonstrate each of these advantages of HR-EBSD analysis. These capabilities open a wealth of opportunities to gain new insights into the details of deformation microstructures and the geological processes that cause and are influenced by them.

1. INTRODUCTION

Electron backscatter diffraction (EBSD) is one of the key techniques for analysing rock microstructures. The diffraction patterns are acquired in a standard scanning electron microscope and therefore EBSD analysis has become routine in many earth science laboratories. The diffraction data provide a diverse range of microstructural datasets relevant to geological questions, including phase identification, crystal (mis)orientation distributions, (sub)grain size, and grain shape, amongst many others. Whilst these data are employed in a wide range of geoscience subdisciplines, they have become particularly central to the study of deformed rocks. In this context, key goals of many microstructural studies are to identify deformation mechanisms that have operated, characterise the microstructures that they generate, and to link both of these to the mechanical properties and deformation histories of the rocks.

Despite its diverse capabilities, conventional EBSD has some key limitations to its ability to characterise subtle intragranular lattice distortions that provide important records of deformation

processes. Crystal orientations are obtained by indexing the Hough transforms of diffraction patterns to a database. However, locating the peaks in Hough space typically limits the precision in misorientation angle between a pair of measurement points to the order of 0.1°. Whilst this angular resolution is sufficient for some purposes, subtle but potentially valuable details of the substructure, such as those associated with low densities of geometrically necessary dislocations (GNDs), can be missed [1]. Furthermore, the precision in misorientation axes decreases with decreasing misorientation angle to the extent that measured misorientation axes can deviate from their true values by tens of degrees for misorientation angles on the order of 1° [2, 3]. Moreover, the Hough transform-based indexing approach does not attempt to recover information on the elastic strain state of the crystal. However, elastic strains and their associated stresses can exert important controls on deformation processes and other microstructural changes.

Recent developments in the materials sciences have largely overcome these limitations by developing an alternative data processing approach. The new approach is based on cross correlation of multiple regions of interest between diffraction patterns to measure the displacement gradient tensor [4]. This tensor can be decomposed into rotations and elastic strains, which can be measured to a precision of 10^{-4}, corresponding to the order of 0.01° [4].

Over the past three years, HR-EBSD has been adapted and applied to geological materials (e.g., [1, 5, 6]. Here, I present a brief overview of the method. Results from geological examples illustrate key points and the potential of the technique to offer new insights into deformation microstructures and the processes that they record and influence.

2. *METHODS: HIGH-ANGULAR RESOLUTION ELECTRON BACKSCATTER DIFFRACTION*

2.1. Development

HR-EBSD developed gradually over the past 25 years or so, but only recently have developments made it suitable for wide-ranging application to the variety of typical rock microstructures. Early works recognised the potential of measuring small shifts of features within EBSD patterns to reveal small lattice rotations and elastic strains [3, 7, 8]. A major development was made by Wilkinson *et al*. [4], who presented a practical and mathematical framework for estimating eight degrees-of-freedom in the displacement gradient tensor, describing rotations and strains, from diffraction patterns obtained on modern megapixel CCD detectors. Subsequent methodological refinements have focussed on improving the accuracy of strain measurement, particularly in the presence of large rotations (e.g., [9-11]). Here, I summarise the key elements of the technique that are necessary to appreciate its applications to geological materials.

2.2. Data Acquisition

As HR-EBSD analysis is largely a post-processing technique most aspects of data acquisition are shared with conventional EBSD. Diffraction patterns are collected from a highly polished specimen surface tilted at 70° towards a phosphor screen and probed with high-energy electrons. As strain resolution is directly proportional to the number of pixels in the diffraction pattern, patterns for HR-EBSD are typically acquired with minimal binning of pixels acquired on a megapixel detector. Images of diffraction patterns are stored for offline HR-EBSD post-processing.

There are two additional data acquisition steps necessary to obtain all the information required for HR-EBSD processing. Shifts in the position of the diffraction pattern due to scanning of the beam across the specimen surface require that a correction is applied to the position of the pattern centre (the point on the phosphor screen closest to the source of the diffraction pattern on the specimen surface). This correction is calculated from data obtained by scanning an undeformed single-crystal standard, in which pattern shifts result only from beam scanning. To apply this correction, the position of the pattern centre must be known as accurately and precisely as possible. Some EBSD systems include an automated routine to determine the pattern centre based on collecting patterns over a range of camera insertion distances, which can be applied before each map acquisition to determine the pattern centre specific to each map.

2.3. Mapping lattice distortion

HR-EBSD data are derived from mapping small distortions within stored images of diffraction patterns. For HR-EBSD, the Hough transform is used only to determine the orientation of a single reference point in each grain. Misorientations between all other points in the grain are determined by cross-correlating regions of interest (ROI) in each diffraction pattern with the corresponding ROI in the pattern from the reference point. A vector, **r**, describing the position of a ROI in the reference pattern, relative to the point from which the pattern is generated, is related to a vector, **r'**, describing the position of the same feature in a test pattern by

$$\mathbf{r}' = (\mathbf{D} + \mathbf{I})\mathbf{r}, \tag{1}$$

where **I** is the identity matrix, and **D** is the displacement gradient tensor [9]. The displacement gradient tensor is defined as

$$\mathbf{D} = \begin{bmatrix} \frac{\partial u_1}{\partial x_1} & \frac{\partial u_1}{\partial x_2} & \frac{\partial u_1}{\partial x_3} \\ \frac{\partial u_2}{\partial x_1} & \frac{\partial u_2}{\partial x_2} & \frac{\partial u_2}{\partial x_3} \\ \frac{\partial u_3}{\partial x_1} & \frac{\partial u_3}{\partial x_2} & \frac{\partial u_3}{\partial x_3} \end{bmatrix}, \tag{2}$$

where x_i is a direction in the crystal and u_i is a displacement in the ith direction [4, 9]. Infinitesimal strains, ε_{ij}, and rotations, ω_{ij}, are represented by the symmetric and antisymmetric parts of **D,** respectively, by Wilkinson *et al*. [4]

$$\varepsilon_{ij} = \frac{1}{2}\left(\frac{\partial u_i}{\partial x_j} + \frac{\partial u_j}{\partial x_i}\right) \tag{3}$$

and

$$\omega_{ij} = \frac{1}{2}\left(\frac{\partial u_i}{\partial x_j} - \frac{\partial u_j}{\partial x_i}\right). \tag{4}$$

If rotations are large, additional processing steps are required to detect the much smaller strain signal. The original approach of Wilkinson *et al*. [4] allows rotations and elastic strains to be recovered up to misorientation angles of ~8°, at which point features in the corresponding regions of interest in the reference and test patterns typically become too dissimilar for accurate analysis. Therefore, Britton and Wilkinson [9, 10] proposed a more robust iterative fitting routine and pattern remapping approach to allow determination of finite rotations (Ω_{ij}) and strains (E_{ij}) up to misorientation angles of ~11°. The elastic strain data, combined with the stiffness tensor of the material, allow calculation of residual stress heterogeneity [12].

2.4. Estimating geometrically necessary dislocation densities in geological materials

Curvature of the crystal lattice results from the presence of geometrically necessary dislocations. Analysis of GNDs can be conducted through the 'dislocation tensor', **α**, using Nye-Kröner analysis (Nye, 1953; Kröner, 1958). Assuming that elastic strain gradients are small relative to orientation gradients, the dislocation tensor can be derived by taking the curl of the lattice rotations,

$$\boldsymbol{\alpha} = \begin{bmatrix} \frac{\partial \Omega_{12}}{\partial x_3} - \frac{\partial \Omega_{31}}{\partial x_2} & \frac{\partial \Omega_{13}}{\partial x_1} & \frac{\partial \Omega_{21}}{\partial x_1} \\ \frac{\partial \Omega_{32}}{\partial x_2} & \frac{\partial \Omega_{23}}{\partial x_1} - \frac{\partial \Omega_{21}}{\partial x_3} & \frac{\partial \Omega_{21}}{\partial x_2} \\ \frac{\partial \Omega_{32}}{\partial x_3} & \frac{\partial \Omega_{13}}{\partial x_3} & \frac{\partial \Omega_{31}}{\partial x_2} - \frac{\partial \Omega_{32}}{\partial x_1} \end{bmatrix}, \tag{5}$$

and can be related to the densities, ρ^s, of s different types of dislocation, each with Burgers vector $\mathbf{b}^s$ and line direction $\mathbf{l}^s$, by [15]

$$\alpha_{ij} = \sum_{s=1}^{s_{max}} \rho^s b_i^s l_j^s \tag{6}$$

From two-dimensional EBSD maps, five of the nine elements of α_{ij} can determined directly, along with the difference between two of the elements ($\alpha_{11} - \alpha_{22}$) [16]. The problem of estimating the densities of each type of GND from the available components of α_{ij} can be set out as

$$\boldsymbol{\rho} = \mathbf{A}^{\mathrm{T}}(\mathbf{A}\mathbf{A}^{T})^{-1}\boldsymbol{\Lambda} \quad (7)$$

where $\boldsymbol{\rho}$ is an s x 1 column vector in which each element represents the density of a particular dislocation type, $\boldsymbol{\Lambda}$ is a 6 x 1 column vector of measured orientation gradients, and $\mathbf{A}$ is a 6 x $s_{\max}$ matrix in which each column contains the dyadic of the Burgers vector and unit line direction of the sth dislocation type [15]. If there are six or fewer dislocation types, then $\boldsymbol{\rho}$ can be calculated directly using an L2 scheme based on eq. 7, which minimizes the misfit between predicted and observed curvatures [1]. This approach has been applied to datasets from olivine [1, 5]. However, if there are more than six possible dislocation types, then $\boldsymbol{\rho}$ is under-constrained and an L1 optimisation scheme is used to find a solution that additionally minimises some other objective variable, such as the total dislocation line energy [15]. The energies of edge and screw dislocations, e_{edge} and e_{screw} respectively, used in the L1 minimisation scheme are in the ratio

$$\frac{e_{edge}}{e_{screw}} = \frac{1}{1-\nu} \quad (8)$$

where ν is the Poisson's ratio. This approach has been applied to quartz, considering 19 dislocation types grouped into six families [6].

3. *RESULTS: GEOMETRICALLY NECESSARY DISLOCATION DENSITIES AND RESIDUAL STRESS HETEROGENEITIES*

3.1. Precision of misorientation angles

HR-EBSD maps of indents in undeformed olivine single crystals demonstrate the improved precision in misorientation angles relative to conventional EBSD. Figure 1 presents an EBSD map of a Berkovich nanoindent in an olivine single crystal and the same dataset reprocessed using the cross correlation-based HR-EBSD approach. The olivine crystal away from the indent is well annealed, such that misorientation angles measured far from the indent result from noise in the measurement techniques. The difference in noise level between the EBSD and HR-EBSD data is evident in the local misorientation maps and is interrogated further in the two profiles. Point-to-point misorientation angles detected along profile A–A' quantify the noise in the misorientation measurements. Misorientation angles determined by conventional EBSD have $2\sigma = 0.12°$, whereas those recalculated by HR-EBSD have $2\sigma = 0.02°$. Profile B–B' demonstrates the impact of measurement noise on the capability of each technique to resolve subtle deformation microstructures. Close to the indent, both the EBSD and HR-EBSD datasets reveal misorientation angles > 1° from the background orientation. However, HR-EBSD provides better characterisation of the subtle orientation gradients further from the indent. For example, at distances along B–B' in the range 35 - 40 μm a clear orientation gradient is evident in the HR-EBSD data but is obscured by noise in the EBSD data.

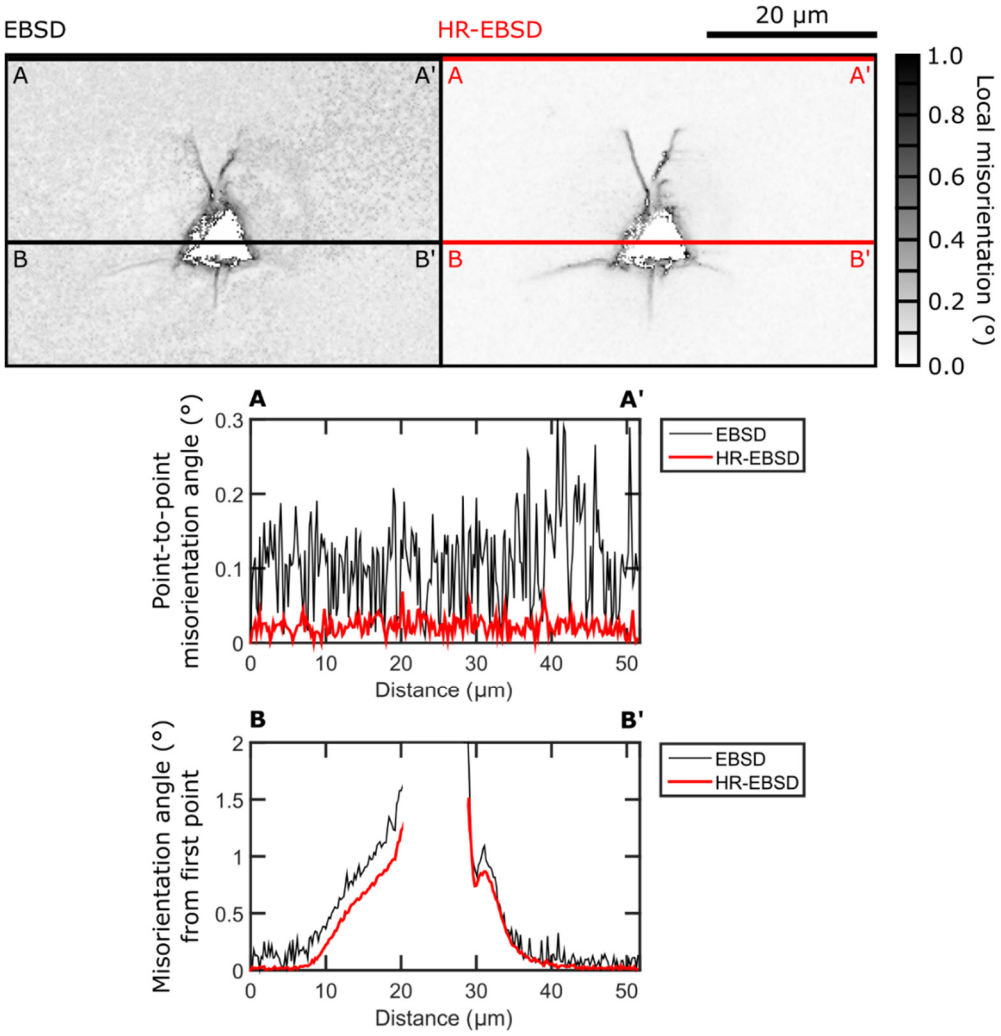

Figure 1. Misorientation data generated by conventional EBSD and HR-EBSD processing of the same diffraction patterns collected across a Berkovich nanoindent in an olivine single crystal. Local misorientation maps present the average misorientation between pixels in a 3x3 pixel kernel centred on each measurement point.

3.2. Misorientation axes and types of geometrically necessary dislocations

3.2.1. Geometrically necessary dislocations in olivine. Maps of an olivine single crystal deformed in uniaxial compression at 1,200 °C reveal the improved determination of GND types offered by HR-EBSD. Figure 2 presents the densities of six dislocation types estimated from conventional EBSD data and HR-EBSD reprocessing of the same diffraction patterns. The different techniques partition dislocation densities differently between the dislocation types. The data from conventional EBSD suggest bands with high densities of [100] screw, [001] screw and (010)[001] edge dislocations. In contrast, the HR-EBSD data reveal higher densities of (001)[100] and (010)[100] edge dislocations. These latter dislocation types are expected to be most abundant based on the deformation temperature and loading orientation of this crystal [5].

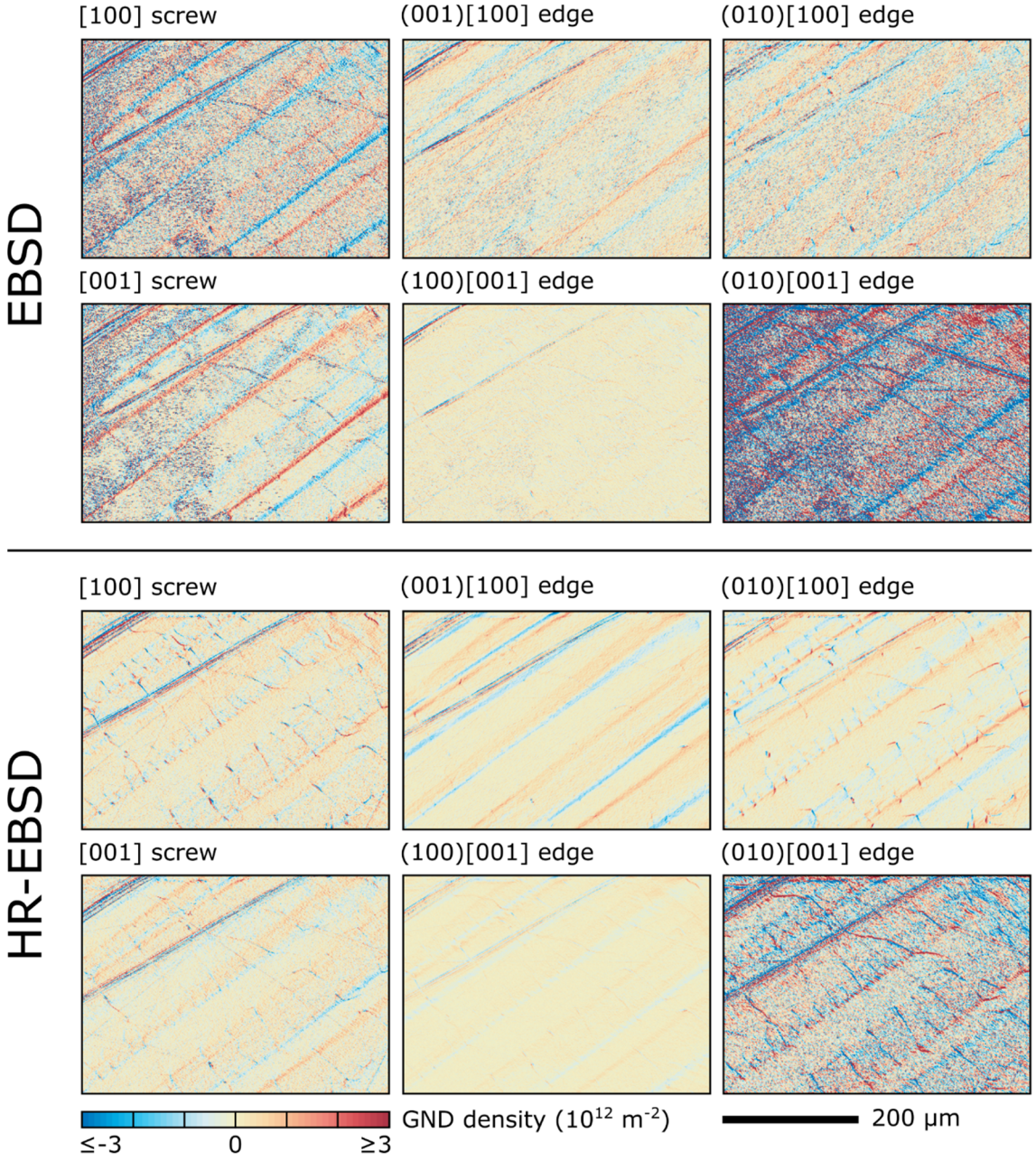

Figure 2. Densities of six types of geometrically necessary dislocation (GND) in a deformed olivine single crystal calculated from conventional EBSD data and HR-EBSD processing of the same diffraction patterns. Modified from Wallis *et al*. [5].

3.2.2. Geometrically necessary dislocations in quartz. Maps of GND types in quartz highlight the challenges of analysing the dislocation content of minerals in the trigonal and hexagonal crystal systems. Figure 3 presents densities of six families of GND types in quartz from the Himalaya [6]. The high dislocation densities define an orthogonal pattern of subgrain boundaries, termed 'chessboard subgrains'. The HR-EBSD data reveal high densities of {*m*}[*c*] edge dislocations, which are an integral component of chessboard subgrain boundaries (e.g., [17]). However, the set of boundaries with traces parallel to those of the prism {*m*} planes appear to contain high densities

of <*a*> screw dislocations. Geometric arguments and independent analyses of chessboard subgrain boundaries indicate that this is an unlikely dislocation arrangement and the (*c*)<*a*> edge dislocations should be expected instead [6]. As screw dislocations are favoured by the energy weighting employed in the L1 minimisation scheme, it is possible that the apparent density of <*a*> screw dislocations may be greater than their true density in this sample. These considerations highlight the need for circumspective interpretation of such results.

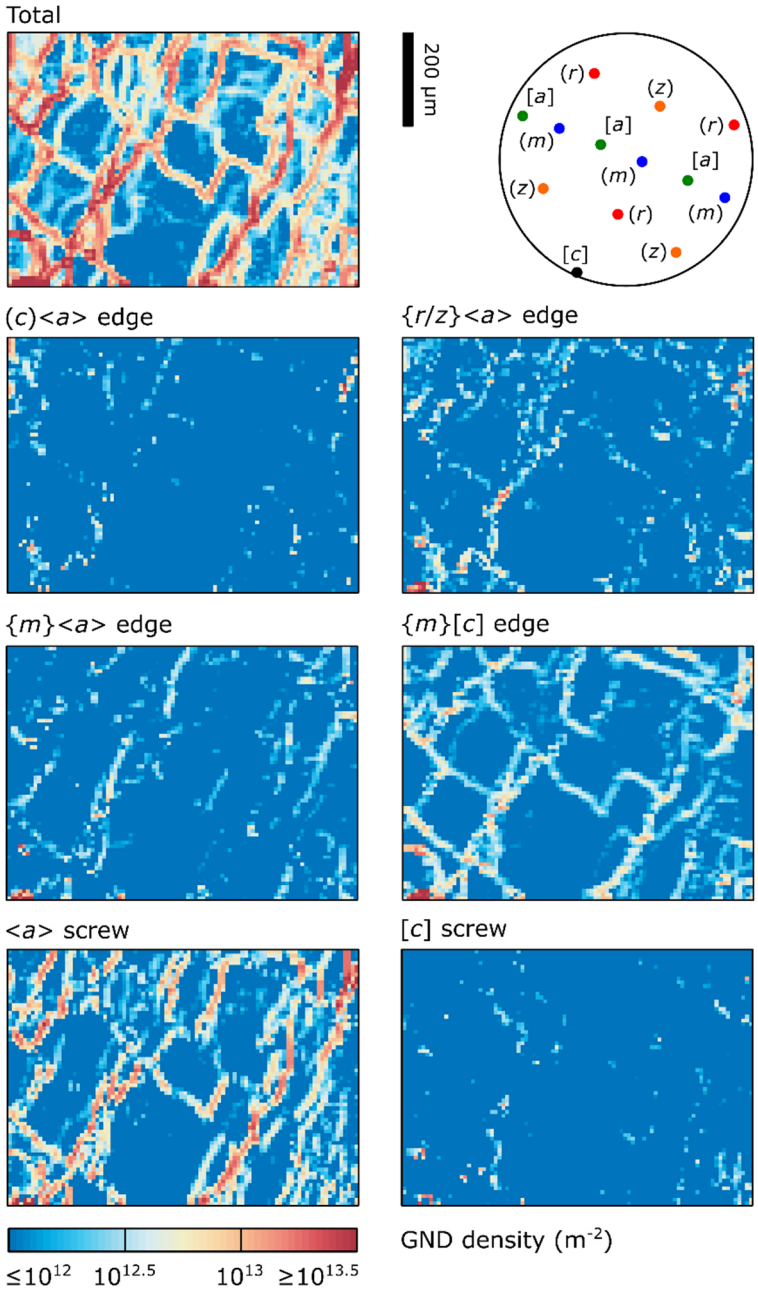

Figure 3. Densities of six families of geometrically necessary dislocations (GNDs) in chessboard subgrain boundaries in quartz. The pole figure displays the orientation of the grain. From Wallis *et al*. [6].

3.3. Elastic strain and residual stress heterogeneities in olivine

HR-EBSD maps of experimentally deformed olivine reveal heterogeneous fields of elastic strain and residual stress. Figure 4 presents maps of stress heterogeneity in an aggregate of olivine deformed at a temperature of 1,250 °C and differential stress of 257 MPa. Each component of the stress tensor is normalised to its mean value within each grain to provide maps of stress heterogeneity relative to the mean stress state of each grain. The intragranular stress fields are highly heterogeneous, commonly varying by over a gigapascal within each grain. Notably, the magnitudes of these stress heterogeneities are several times greater than the externally applied differential stress during deformation and therefore reveal local stress concentrations.

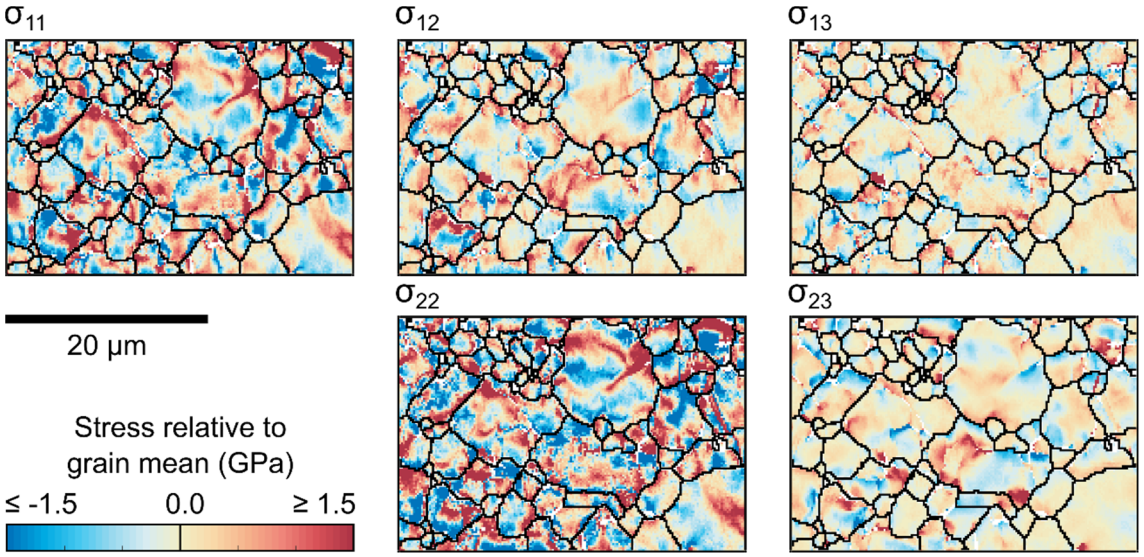

Figure 4. Maps of each component of the symmetrical stress tensor (σ_{ij}) normalised to the mean value of each component in each grain, i.e., maps of intragranular stress heterogeneity. The σ_{33} component is not plotted as it is assumed to be zero during the calculation of the ε_{33} component of the strain tensor, based on relaxation due to sectioning.

4. DISCUSSION: APPLICATION OF HR-EBSD TO GEOLOGICAL MATERIALS

Initial applications of HR-EBSD to geological materials have demonstrated its capability to achieve dramatically improved precision in misorientation angles (Fig. 1) (and hence GND density) and misorientation axes (and hence GND types, Fig. 2) compared to conventional EBSD [1]. Moreover, HR-EBSD provides the new opportunity to measure elastic strain and residual stress heterogeneities from EBSD data on minerals (Fig. 4; [5]). These initial datasets demonstrate that the technique can provide data on geological materials of comparable quality to those obtained from semiconductors and metals (e.g., [4, 12, 15]), despite potential differences in pattern quality, symmetry, and dislocation types.

The application of HR-EBSD to geological materials involves benefiting from lessons learned in the materials sciences along with making new developments. For example, the lattices of geological minerals deformed at high temperature often exhibit large intragranular rotations due to wide-spread subgrain development. The orientations of quartz in Fig. 3, for instance, vary by approximately 11°. Two recent developments have enabled HR-EBSD analysis of such microstructures. Britton and Wilkinson [9] proposed a robust iterative fitting scheme to determine the displacement gradient tensor that down-weights less reliable shifts in some ROIs that may occur with large rotations. Similarly, Britton and Wilkinson [10] developed a two-step pattern remapping approach, bringing the test pattern into a similar orientation to the reference pattern, allowing elastic strain measurements in the presence of rotations up to 11°. This method relies upon accurate knowledge of the pattern centre and highlights the importance of careful acquisition procedures, such as employing a camera-stepping routine (Section 2.2). Nonetheless, these complex microstructures also offer benefits for data collection. Work on both copper [18] and olivine [1] has demonstrated that binning of pixels in the detector's CCD camera has negligible impacts on estimated GND density (but not necessarily on elastic strain) associated with rotations of several degrees. Increased binning improves the speed of both data acquisition and processing.

The varied symmetries of geological materials and their slip systems present a new choice of methods for estimating GND density. The use of L1 schemes that minimise a variable such as total dislocation line energy, typically applied to cubic and hexagonal metals [12, 15], can be explored for minerals such as quartz, calcite, and garnet, which also exhibit more than six potentially active dislocation types (Fig. 3; [6]). Some minerals, for which only six appropriate dislocation types need be considered, such as olivine (Fig. 2; [1, 5]), can be analysed using a simple L2 solution to Eq. 7 to estimate the best-fit densities of each GND type. Other approaches to analysing GND content are available, such as the weighted Burgers vector of Wheeler *et al*. [19] and could be applied to HR-EBSD rotation data to benefit from high-precision misorientation measurements.

Initial HR-EBSD measurements of residual stresses in rocks have revealed surprising magnitudes of intragranular stress heterogeneity. Intragranular stress states have been demonstrated to vary by 100s MPa in single crystals [5] and over 1 GPa in aggregates (Fig. 4). These magnitudes are comparable to those observed in metals and are well justified based on the stresses associated with dislocation content (e.g., [20]). A wide variety of additional sources can potentially contribute to stress heterogeneity in rocks, which have generally undergone some degree of deformation, cooling, and decompression. This complexity raises a need to develop new methods for interpreting the causes of stress heterogeneity based on HR-EBSD datasets.

The capabilities of HR-EBSD open a wealth of opportunities for new investigations of geological processes based on subtle aspects of deformation microstructures in rocks. Possibilities include the mechanisms, external conditions, and internal mechanical states of deformation; changes in pressure and temperature, and reaction and crystallisation processes in metamorphic and igneous rocks; and compaction and mineral growth in sedimentary and diagenetic contexts.

5. CONCLUSIONS

HR-EBSD is a breakthrough method for analysing the microstructures of geological materials in new levels of detail. The precise misorientation, GND density, elastic strain heterogeneity, and residual stress heterogeneity measurements offer new depths of insight into the distorted internal states of mineral structures and the processes that have influenced them. HR-EBSD in the geosciences benefits from, and builds upon, major advances achieved in the materials sciences, as part of an ongoing drive to establish the links between microstructure, material properties, and external processes.

6. ACKNOWJEDGEMENTS

The author thanks Lars Hansen for the inspiration and support to carry out this work. Thanks also to Angus Wilkinson and Ben Britton for their work on the development of the HR-EBSD technique and the code that provided the basis for the present work. David Kohlstedt and Andrew Parsons generously provided samples for HR-EBSD analysis. This work was supported by the Natural Environment Research Council Grant NE/M000966/1.

7. REFERENCES

[1] Wallis D, Hansen L N, Britton T B and Wilkinson A J 2016 Geometrically necessary dislocation densities in olivine obtained using high-angular resolution electron backscatter diffraction. *Ultramicroscopy* **168** 34-45

[2] Prior D J 1999 Problems in determining the misorientation axes, for small angular misorientations, using electron backscatter diffraction. *J. Microscopy* **195** 217-225

[3] Wilkinson A J 2001 A new method for determining small misorientations from electron back scatter diffraction patterns. *Scripta Materialia* **44** 2379-2385

[4] Wilkinson A J, Meaden G. and Dingley D J 2006 High-resolution elastic strain measurement from electron backscatter diffraction patterns: New levels of sensitivity. *Ultramicroscopy* **106** 307-313

[5] Wallis D, Hansen L N, Britton T B and Wilkinson A J 2017 Dislocation interactions in olivine revealed by HR-EBSD. *J. Geophys. Res.: Solid Earth* **122** 7659-7678

[6] Wallis D, Parsons A J and Hansen L N 2017 Quantifying geometrically necessary dislocations in quartz using HR-ESBD: Application to chessboard subgrain boundaries. in: *Back to the future: 40 years of structural geology and beyond; Journal of Structural Geology 40th Anniversary Special Issue*. (Hippertt J; Ed.) DOI: 10.1016/j.jsg.2017.12.012

[7] Troost K Z, van der Sluis P and Gravesteijn D J 1993 Microscale elastic-strain determination by backscatter Kikuchi diffraction in the scanning electron microscope. *Appl. Phys. Lett.* **62** 1110-1112

[8] Wilkinson A J 1996 Measurement of elastic strains and small lattice rotations using electron back scatter diffraction. *Ultramicroscopy* **62** 237-247

[9] Britton T B and Wilkinson A J 2011 Measurement of residual elastic strain and lattice rotations with high resolution electron backscatter diffraction. *Ultramicroscopy* **111** 1395-1404

[10] Britton T B and Wilkinson A J 2012 High resolution electron backscatter diffraction measurements of elastic strain variations in the presence of larger lattice rotations. *Ultramicroscopy* **114** 82-95

[11] Villert S, Maurice C, Wyon C and Fortunier R 2011 Accuracy assessment of elastic strain measurement by EBSD. *J. Microscopy* **233** 290-301

[12] Britton T B and Wilkinson A J 2012 Stress fields and geometrically necessary dislocation density distributions near the head of a blocked slip band. *Acta Materialia* **60** 5773-5782

[13] Nye J F 1953 Some geometrical relations in dislocated crystals. *Acta Metallurgica* **1** 153-162

[14] Kröner E 1958 Continuum theory of dislocations and self-stresses. *Ergebnisse der Angewandten Mathematik* **5** 1327-1347

[15] Wilkinson A J and Randman D 2010 Determination of elastic strain fields and geometrically necessary dislocation distributions near nanoindents using electron backscatter diffraction. *Philosophical Mag.* **90** 1159-1177

[16] Pantleon W 2008 Resolving the geometrically necessary dislocation content by conventional electron backscattering diffraction. *Scripta Materialia* **58** 994-997

[17] Kruhl J H 1996 Prism- and basal-plane parallel subgrain boundaries in quartz: a microstructural geothermobarometer. *J. Metamorphic Geology* **14** 581-589

[18] Jiang J, Britton T B and Wilkinson A J 2013 Measurement of geometrically necessary dislocation density with high resolution electron backscatter diffraction: Effects of detector binning and step size. *Ultramicroscopy* **125** 1-9

[19] Wheeler J, Mariani E, Piazolo S, Prior D J, Trimby P and Drury M R 2009 The weighted Burgers vector: a new quantity for constraining dislocation densities and types using electron backscatter diffraction on 2D sections through crystalline materials. *J. Microscopy* **233** 482-494

[20] Jiang J, Britton T B and Wilkinson A J 2013 Mapping type III intragranular residual stress distributions in deformed copper polycrystals. *Acta Materialia* **61** 5895-5904